

Robust Real-Time Chaos Detection from Measurement Data

CARLOS M. N. VELOSA, KOUAMANA BOUSSON

Department of Aerospace Sciences

University of Beira Interior

6201-001 Covilhã

PORTUGAL

carlosvelosaeng@hotmail.com, k1bousson@yahoo.com

Abstract: - The ability to distinguish between chaotic from regular dynamics is not a trivial task and the fact that noise cannot be avoided in real physical systems makes the problem even more challenging. Chaos becomes highly unpredictable after a very short period of time as a random-like motion that traditional detection techniques may fail, especially when measurement noises are taken into consideration. The present paper proposes a new algorithm to detect chaotic modes automatically (without any model), in real-time and in the presence of noise. The key idea behind the detection lies in the fact that a single component of a chaotic trajectory tends to exhibit an infinite number of local maxima at different time-instants. Using an auxiliary system acting as a denoiser and resorting to simple mathematical operations, it is established a parameter that characterizes the type of motion based on a specified threshold. Numerical simulations are presented to validate the effectiveness and robustness using three applications: a butterfly-shaped system identical to the celebrated Lorenz system; and two aerospace systems related to the attitude motion of spacecraft. The results show that the distinction is very clear and the detector is effective even for relatively low Signal-to-Noise Ratios. The proposed detector is easily-implementable and very efficient from the computational viewpoint as opposed to other tools of chaos detection.

Key-Words: - Chaos, Chaos detection, Robust detection, On-line detection, Spacecraft, Attitude motion.

1 Introduction

Chaotic systems have attracted significant attention from researchers over the last two decades and there has been since then a large effort in attempting to develop and improve techniques of chaos detection, [1]–[8]. Chaos, as well-known, may be desirable or not depending on the purpose of the application. In applications such as combustion, it is desired because it provides a better fuel-air mixture that leads consequently to a better performance. Random number generators and sources of chaotic signals used as carrier frequencies in telecommunication systems are, on the other hand, the most classic examples. Another interesting example where it may be useful occurs in spacecraft manoeuvres. The ‘main’ characteristic of chaos - *high sensitivity to initial conditions* - may be used in a clever way to perform orbital manoeuvres at a very low cost given that small initial deviations lead to completely different trajectories. A proof of that was the manoeuvre achieved with the satellite ISEE-3/ICE (*International Sun-Earth Explorer / International Cometary Explorer*), where once ended its first mission, engineers resorted carefully to that sensitivity to transfer the satellite to another orbit

with a minimum expenditure of fuel, continuing there posteriorly its second mission, [9]–[11]. Contrariwise, in aerodynamics, chaos (turbulence) is no longer desired because it increases drastically the drag of an aircraft, leading naturally to higher operational costs. In a communication satellite, a chaotic attitude motion is also not desired since the antenna must be pointed toward a specific target. Mechanical and structural systems are, on the other hand, typical examples where chaos should be avoided because chaotic vibrations can lead to a fatigue failure. However, desirable or not, uncertainties are surely not desired in engineering problems, and in that sense the detection theory plays an important role. A dynamical system may be designed, through the appropriate choice of its parameters, to not exhibit a chaotic behaviour. Nevertheless, there is no guarantee that chaos will not occur, because any nonlinear system may come to exhibit chaotic motions if the system is subject to disturbances with specific characteristics, even if it has been designed to exhibit a regular motion, [12], [13]. Be able to detect unexpected transitions from regular- to chaotic- behaviours is for this reason

extremely crucial because only then control actions can be properly applied. Several are the techniques that can be found in the literature for the control and synchronization of chaotic systems, [12], [14]–[22].

The purpose of the present paper is to propose an algorithm for automatic and real-time chaos detection from time series corrupted with noise with relatively low Signal-to-Noise Ratios (SNR). The work is motivated by the fact that most of the existing tools are based on the model of the system or in noiseless time series, and, on the other hand, also because many of such techniques are only useful if applied offline. Few are the techniques available to detect automatically the presence of chaos, and in that sense it is extremely necessary to find effective solutions even in the presence of disturbances, once there are highly demanding applications, such as aerospace and aeronautical systems (e.g.: satellites, aircraft wings, helicopter rotors, etc.), that may exhibit undesirable chaotic motions that if are not detected and suppressed ‘immediately’ can lead to catastrophic scenarios.

The rest of the paper is organized as follows: section 2 presents a review of the existing tools for analysis and detection of chaotic vibrations in deterministic systems with special emphasis on their weaknesses; section 3 specifies the problem to be solved; in section 4, a solution to the problem, which is a new method based in one of the main characteristics of chaos, is proposed; in section 5, numerical simulations are performed to validate the effectiveness and robustness of the detector; section 6 presents a discussion about the results; and section 7 completes lastly the paper with concluding remarks and suggestions for future extensions of the method.

2 Background

Chaos is typically referred as a complex, irregular, and unpredictable random-like motion, which is highly sensitive to initial conditions and that results from the superposition of an infinite number of unstable periodic motions produced by deterministic nonlinear system, [23], [24]. In a chaotic system, despite being governed by well-defined dynamical laws, and most of the times even with a relatively simple structure, two trajectories initiated very close to each other become completely different after a very short period of time. The phenomenon has been intensely called of *butterfly effect*, portraying the fact that a small disturbance induced by a butterfly flapping its wings in a particular place of the planet might ultimately cause a hurricane a few

days later in another part of the planet, [25]. Chaotic systems are also extremely sensitive to parameter changes. A given system may be operating in a well regular regime and at the tiniest variation in one of its parameters come to exhibit a chaotic behaviour, and hence a completely different regime than desired. Another characteristic of the chaotic motion is that it presents in its phase-space a geometric object of fractal structure designated by *strange attractor*. In a *strange attractor*, the trajectories are confined to a bounded region, never repeat the same path twice, are recurrent, and all trajectories in its vicinity are attracted by it. The recurrence property means that, given enough time, the trajectory returns sooner or later arbitrarily close to any point of the phase-space. As previously mentioned, chaos is an unpredictable type of motion, but it should be noted that it is unpredictable only after a specific time (very short) from the beginning. This is one of the characteristics that distinguish it from a true stochastic process, since a stochastic process is unpredictable at any time. On the other hand, although the trajectories do not follow any type of pattern, the chaotic behaviour is governed entirely, or at least in part, by deterministic dynamical equations, as opposed to purely stochastic processes which can only be described by statistical properties. Another interesting characteristic of chaos is extracted in the frequency domain. A chaotic signal is characterized by having a continuous frequency spectrum, broadband, but bounded, and such characteristic is what differentiates it from periodic-, quasi-periodic- and stochastic- signals. Note that, if on one hand the existence of many frequencies distinguishes it from periodic signals, a bounded spectrum distinguishes it from stochastic signals, since the latter are characterized by having distributed frequencies over the entire spectrum. As stated also before, the chaotic behaviour may arise only in nonlinear systems. Theoretically, it is impossible that a (finite-dimensional) linear system comes to exhibit chaotic vibrations, since a linear system is one in which if a change in a particular variable at some initial time produces a change in the same or in another variable at some posterior time, a change n times larger at the same initial time produces a change n times larger at the same posterior time. Chaos is induced by nature due to the nonlinearities, because only then the change observed at a specific time is not proportional to the change at the initial time. Mathematically, the chaotic motion is characterized by local instability, globally limited trajectories, and by a random-like motion as already stated. However, it is well-known that there is no

universally accepted definition and because of that chaos is defined as having the following set of characteristics, instead of a general definition: 1) deterministic; 2) nonlinear; 3) high sensitivity to initial conditions; 4) high sensitivity to parameter changes; 5) bounded phase-space; 6) associated to a fractal structure/strange attractor; 7) unpredictability of the trajectories beyond a very short period of time; 8) recurrence/ergodicity; and 9) a continuous frequency spectrum, broadband, and bounded.

2.1 Techniques of Chaos Analysis and Detection

Usually, the first clue that a certain system exhibits a chaotic behaviour is given through observation over the time of the system outputs (*time histories*), and through representation of its coordinates in one or more plots, that is, analysing the system *phase-space* and/or *phase-planes*. Contrary to what happens when the system exhibits a regular behaviour, where it is evident an equilibrium point, a periodic- or a quasi-periodic- orbit, the observed motion does not reveal any periodicity or repeating patterns, and in some cases the trajectory toggles between equilibrium states oscillating momentarily around each of these states. A chaotic motion is thus associated to a fractal structure, and it exists when the phase-space shows a strange attractor. However, both the *time history* as the *phase-space* analysis are merely indicative. A visual inspection is not sufficient to characterize the system dynamics. The motion may own more than one main period, as is the case of a chaotic motion, and in this condition distinguish a quasi-periodic motion of many periods from a chaotic motion is not so easy, if not even impossible. Furthermore, the fact that the *phase-space* exhibits a strange attractor may not imply necessarily the presence of chaos once not all strange attractors are chaotic, [26], [27].

Poincaré sections are very useful when it comes to evaluating the qualitative behaviour of continuous systems. By creating one or more sections each one transverse to the flow at a given point, and analysing the intersection of the orbits with each of these sections, a continuous system described by n state variables is transformed into a discrete system of $n - 1$ variables which makes clearer the perception of its dynamics. An orbit of period one is thus characterized by a single point, an orbit of period two by two points, and so forth until arises a cloud of points indicating a chaotic motion. *Poincaré sections* allow to distinguish periodic-, quasi-periodic-, and chaotic- vibrations. However,

Poincaré sections are quite sensitive to the noise inevitable in real-world systems. Influenced by noise, each orbit can be slightly deviated at the exact instant it crosses the section, causing the appearance of numerous points and inducing in the presence of chaos, when the motion can be in fact periodic. Noise reduction techniques should be thus applied to minimize the effects of noise and if their characteristics are known the designer may consider small clouds of points as individual points. It is a strategy that simplifies the analysis, but that is useful only for quasi-periodic vibrations and when the periods are sufficiently distant from each other. Additionally, the flow may not have a global section, because it would have to be transversal to all possible orbits, and an inappropriate choice may cause the appearance of only a few points when in fact there may exist much more.

The chaotic behaviour can be originated by different routes. *Period-doubling*, *torus breakdown* and *intermittency* are the three most common, and for many systems the *period-doubling* is a very common route, [23], [28]–[31]. In this in particular, the period increases in powers of two as one of the parameters is increased (or decreased), and as a result, the motion is said to be (multi)periodic when the system exhibits a finite number of states or chaotic when it exhibits an infinite number of states. The *bifurcation diagram* is a graphical tool based on this assumption that allows determining for which values of parameters occurs the chaotic behaviour. *Bifurcation diagrams* become a very useful tool when analysing nonlinear systems, insofar as they show the overall dynamics as a function of the parameters. However, the analysis has to be carried out offline, requires knowledge of the exact mathematical equations, depends on the human visual acuity to determine the type of behaviour, and only can predict the *period-doubling* route to chaos.

In addition to the absence of a regular behaviour, chaotic systems are characterized essentially by high sensitivity to initial conditions: two trajectories initiated very close to each other move away over the time until lose any type of correlation between them. Based on this statement, the *Lyapunov exponents* characterize the rate of exponential divergence/convergence of nearby system trajectories, and as a result the dynamics is said to be chaotic when there is at least one positive exponent, [32]. The *largest Lyapunov exponent* is thus the most important number and allows to distinguish, not only a chaotic- from a regular-signal, but also a purely deterministic- from a stochastic- signal given the latter is characterized by a positive but infinite *exponent*, [33]. The *largest*

Lyapunov exponent may be estimated from time series, and for that purpose the works of [32], [34]–[38] are the most relevant that can be found in literature. However, the method is not robust enough and it may fail under certain conditions. Due to the inevitable presence of noise in real systems, the largest exponent may result in a positive value, indicating thus the presence of chaos when the system exhibits actually a regular behaviour. Filtering techniques can be obviously applied in order to reduce the effects of noise, but there are also other drawbacks, among which stand out the reasonable/high computational effort demanded and the fact that it requires a time series with a sufficiently large number of samples.

As opposed to a periodic- or multi-periodic-signal, where a *spectral analysis* reveals well-defined frequencies, a chaotic signal is characterized by having a continuous frequency spectrum, broadband, but nonetheless limited, [23], [31], [33]. On one hand, the existence of many frequencies is a characteristic that distinguishes a chaotic- from a periodic- signal, and, on the other hand, a bounded spectrum allows to distinguish a chaotic- from a stochastic- signal because this latter presents distributed frequencies throughout the spectrum. If the time series under analysis is purely deterministic, chaos detection through a frequency spectrum observation is relatively simple. However, when the time series is corrupted with noise, the *spectral analysis* may fail because it becomes difficult to distinguish a chaotic- from a non-chaotic- signal, given that the *Fourier Transform* exhibits frequencies in the entire spectrum due to the presence of noise. Filtering techniques shall be applied before the use of this tool to minimize the effects of noise. Nevertheless, a *spectral analysis* must be used with some precaution because, even when the signal is noise-free, it may occur that the distinction between a quasi-periodic signal of many periods and a chaotic signal is not so clear due to the presence of several frequencies very close to each other.

For the cases where the distinction between a chaotic signal and a quasi-periodic signal of many periods very close to each other is not so clear, the *autocorrelation function* is a very useful tool, [23], [33]. Related to the *Fourier Transform*, it allows distinguishing a periodic- from a chaotic- or a stochastic- signal. When the time series is periodic in time, the *autocorrelation function*, which relates the time series with the same time series with a lag, is periodic in the lag. When the time series is generated through a deterministic chaotic system, the *autocorrelation function* decays exponentially to

zero as the lag increases. If the time series is stochastic, the *autocorrelation function* tends to zero as the lag increases, but with a decay rate that depends on the properties of the process. The *autocorrelation function* allows distinguishing a periodic- from a chaotic- or a stochastic- signal. Nevertheless, it is not powerful enough to distinguish a chaotic- from a stochastic- signal since the function tends to zero in both cases.

The *Melnikov analysis* is an analytical tool used in many cases to predict the occurrence of chaos in nonlinear systems subject to small disturbances. In its classical form, the method was developed for time-varying smooth bi-dimensional systems, assuming knowledge of a homoclinic orbit associated to a saddle point of the unperturbed system. The presence of chaos is then declared if the *Melnikov function* presents at least a simple zero, [39], [40]. Analytical approaches are no doubt more powerful than numerical ones, and in that sense the methods based on the *Melnikov theory* are quite reliable. Nevertheless, the methods are not ideal and have hence some relevant drawbacks, [41]–[43]: 1) they can predict only the homoclinic/heteroclinic chaos; 2) for general disturbances, the detection may fail; and 3), they are associated to cumbersome algebraic computations. In addition, the methods based on Melnikov are analytical, requiring therefore the exact knowledge of the model as well the exact knowledge of the disturbances, and in that sense they are not appropriate at all to detect chaos in real-world applications because the models are known very often only with a degree of certainty and the disturbances are almost always unknown.

Since chaos is characterized by unpredictability of the system trajectories and by critical sensitivity to initial conditions, Awrejcewicz and Dzyubak, [7], proposed a numerical method to trace the domains of chaoticity and regularity of any nonlinear system governed by ordinary differential equations. Entitled by *analysis of wandering trajectories*, the method compares, at each step, the error between two trajectories started with initial conditions very close to each other with a specified threshold, and that comparison/test allows determining the chaoticity regions as functions of the parameters. It has been proven that the method is much simpler and faster from the computational point of view than the well-known *Lyapunov exponents*, [41]. However, the *analysis of wandering trajectories* requires a priori knowledge of the model, because only thus it can be integrated starting from two initial conditions, and because of this it cannot be used to detect chaos from time series. On the other hand, even if the model is known, any real-world system is almost

always subject to unknown uncertainties which may change its behaviour considerably, and due to such uncertainties the trajectories obtained by integration of the model may not describe accurately the true dynamics of the real system.

The method proposed by Poon and Barahona, [6], allows the detection of chaos from time series even when the series is short or is corrupted with measurement noise, and in that sense their work stands out among all other numerical techniques. Designated by *Noise Titration*, the method consists in adding successively small quantities of noise to the time series until the nonlinearity of a specified autoregressive Volterra model be completely destroyed. Then, the maximum amount of noise required to destroy that nonlinearity indicates whether the time series is chaotic or not. The method is considered superior to the *Lyapunov exponents*, [44], [45], and although it seems to be at first glance an ideal approach to detect chaos, it has been reported several cases where the detection actually fails, [46]. On the other hand, the method requires a successive addition of small amounts of noise, a procedure which makes the detection process time-consuming and that is obviously not desired.

Gottwald and Melbourne, [2], [5], developed a very interesting method for chaos detection from time series that works effectively even in the presence of low levels of measurement noise. Designated by *0-1 Test*, it is a binary test that distinguishes between chaotic from non-chaotic data based on a measure of the asymptotic growth rate of the mean square displacement between two functions. The theory behind the method is indeed interesting and that brings several favourable points face to the other detection tools. It is applicable to a single time series, whereby it does not require the model of the system; it does not require any visual aids in the decision process, meaning that chaos can be detected automatically; and it allows an online detection if the length observation window is not too large. However, the *0-1 Test* is formulated under the hypothesis of deterministic signals, and in that sense it can only detect the so-called pure deterministic chaos. Stochastic signals are identified as being chaotic when actually they are not. On the other hand, the method may fail for some deterministic systems or when sampling frequency to get the time series is not appropriate.

Very recently, Fouda et al., [1], formulated a method capable of discerning clearly between chaotic-, periodic- and quasi-periodic- motions. Entitled by *Three-State Test (3ST)*, the method is based on a function that measures the ability of a

given dynamical system generates new patterns as the time increases. As opposed to the *0-1 Test*, which only distinguishes between chaotic- from non-chaotic- signals, the *3ST* is clearly more efficient from the computational point of view, and in that sense it would be an excellent test for detection in real-time. Nevertheless, like any other chaos detection method, the *3ST* is highly sensitive to small changes in the input, whereby it is only effective for a level of noise sufficiently small. Another drawback is related to size of the observation window. If the number of samples is not sufficiently representative, the test tends to confuse quasi-periodic motions to weak chaos. Lastly, but also important, even that filters are applied to reduce the level of noise, the test is applicable only to discrete-time systems and requires yet an extension for the case of continuous-time systems.

In addition to the aforementioned techniques, approaches based on different concepts of detection have been also explored, [3], [4], [47]–[49]. However, the authors have noticed that the methods proposed so far have some common drawbacks that make them inappropriate for a detection in real-time or in noisy environments. It occurs that for some demanding applications as in the aerospace and aeronautical fields, the presence of chaos must be detected satisfying certain requisites: 1) chaos must be detected in an automatic way; 2) it should be detected from time series because the exact model of the system may not be known with accuracy and/or there may exist disturbances of unknown properties; 3) it should be detected preferentially from short time series because it is desirable to reach a detection as fast as possible in order to trigger a control action; 4) the detector must be robust against measurement noise once the noise cannot be avoided; and lastly, 5), the detection algorithm should not be time-consuming since the problem requires a real-time solution.

3 Problem Statement

Consider a continuous-time dynamical system governed by a set of ordinary differential equations and assume that only one of its outputs is available for measurement. That is, a system described by the following mathematical model:

$$\begin{aligned} \dot{x} &= f(x, u, t) + g(x, t) \\ y &= h(x, u, t) \\ y_{obs}[n] &= c^T y[n] + w[n] \end{aligned} \quad (1)$$

where $x \in \mathbb{R}^n$ denotes the state vector, $y \in \mathbb{R}^q$ the output vector, $u \in \mathbb{R}^m$ the control vector, f, g, h three vector-valued nonlinear functions, t the time, and $\dot{x} = dx/dt$. The third equation, $y_{obs} \in \mathbb{R}$, denotes the unique observable output of the system, which is measured with a specified constant sampling frequency, $f_s = 1/dt$, and takes into account Additive White Gaussian Noise (AWGN), w , representing the noise introduced inevitably by the measurement sensor or resulting from a given data fusion algorithm. $c \in \mathbb{R}^q$ denotes the output vector. In the first equation, g may be unknown, it represents possible unmodeled dynamics, parameter uncertainties, and/or external time-varying disturbances.

Since model (1) is described by nonlinear functions, it may exhibit, as well-known: an equilibrium state; a periodic motion; a quasi-periodic motion; or a chaotic motion, depending on the values of the parameters and on eventual external disturbances if they meet specific characteristics (frequency and amplitude). The chaotic motion may be desirable or not depending on the application. However, for most dynamical systems a chaotic motion is not desired because it can lead to a catastrophic scenario. Then, the problem to be solved consists in formulating an automatic chaos detector capable of detecting the occurrence of chaotic modes in real-time, assuming that y_{obs} is the unique available information and that it is corrupted with measurement noise w .

4 The Proposed Algorithm

Consider a continuous-time, time-invariant, bi-dimensional and stable auxiliary linear system, described as follows, $\dot{z} = Az + by_{obs}$:

$$\begin{bmatrix} \dot{z}_1 \\ \dot{z}_2 \end{bmatrix} = \begin{bmatrix} a_{11} & a_{12} \\ a_{21} & a_{22} \end{bmatrix} \begin{bmatrix} z_1 \\ z_2 \end{bmatrix} + \begin{bmatrix} b_1 \\ b_2 \end{bmatrix} y_{obs} \quad (2)$$

where $z \in \mathbb{R}^2$ denotes the state vector, $y_{obs} \in \mathbb{R}$ the control variable that corresponds to the signal under analysis, $A \in \mathbb{R}^{2 \times 2}$ an Hurwitz state matrix, that is, a matrix whose all its eigenvalues are in the open left half plane, $\text{Re}[\lambda_i(A)] < 0$, $i = 1, 2$, and $b \in \mathbb{R}^2$ the control vector, with $b \neq 0$.

Let equation (2) be solved using an appropriate method (e.g.: Euler, Runge-Kutta) step-by-step as each new measurement $y_{obs}(n)$ is available, that is, with a step size = dt . Consider then a sliding observation window of length N points comprising

the time-instants t_1, t_2, \dots, t_N for which z_2 presents local maxima, where the oldest t_i is discarded each time a new maximum is found and the newest t_j is introduced based on a FIFO (First-In, First-Out) philosophy. Compute now the Δt 's, $\Delta t_n = t_{n+1} - t_n$, between each two consecutive local maxima and obtain a time series of $N - 1$ points. In the absence of noise, there will be a finite number k of repeated Δt 's for the case of a regular time series, no matter how many periods the signal has, and an 'infinite' number k of different Δt 's for the case of a chaotic time series. This is the key idea behind the new chaos detector. Chaos is characterized by a highly unpredictable motion which displays infinite local maxima at different time-instants. Fig. 1 depicts the observation window for a regular signal $z_2(t)$.

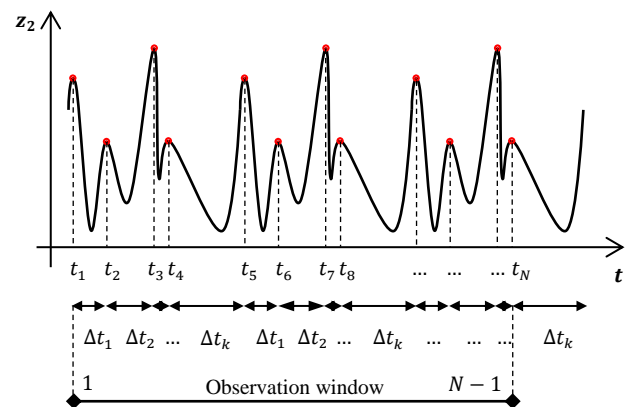


Fig. 1. Determination of the observation window: time-instants for which z_2 has local maxima.

The next step consists in sorting the Δt 's in ascending order (\nearrow). This yields a time series in the form of stairs (finite k), as depicted in the upper plot of Fig. 2, for the case of a regular signal z_2 , or a time series with the appearance of an exponential function ('infinite' k) for the case of a chaotic z_2 . Then, computing the $\Delta(\Delta t)$'s, $\Delta(\Delta t)_n = \Delta t_{n+1} - \Delta t_n$, one obtains a time series of $N - 2$ points containing the variations between different stairs, or, in another words, the numerical derivative of that time series. It occurs that there will be $k - 1$ different stairs, where k is a finite number for a regular z_2 and an 'infinite' number (or at least very large) for a chaotic z_2 . It is noteworthy that the number of different stairs depends exclusively on the complexity of z_2 since there is no any relationship with the size of the observation window. The more unpredictable is the trajectory the more distinct stairs will exist. The last step consists in discarding the isolated peaks, that is, the points whose values immediately before and after

them are both zero. Fig. 2 portrays the entire procedure taking into account a regular signal z_2 .

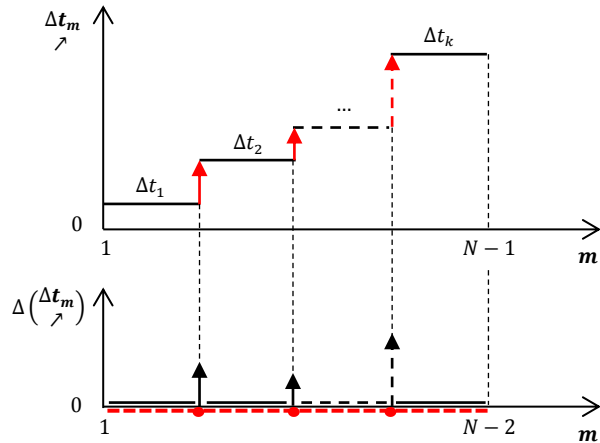


Fig. 2. Representation of Δt_m in ascending order (λ) – upper plot; and representation of $\Delta(\Delta t_m)$ (black/solid line) and $\Delta(\Delta t_m)$ with isolated peaks removed (red/dashed line) – lower plot.

By carrying out this procedure for each observation window, chaos is easily distinguished from the regular motion. The resulting time series (a vector, computationally speaking) is a null vector if z_2 is a regular signal or a vector where most of its points are above the zero line if z_2 is a chaotic signal. In order to detect automatically this difference, without resorting to any visual aids, one defines the following ratio:

$$R = \frac{n^{\circ} \text{ of points greater than zero}}{n^{\circ} \text{ of points equal to zero}} \quad (3)$$

Thus, a regular motion (periodic / multi-periodic) is characterized by a ratio $R = 0$ and a chaotic motion by a ratio $R \gg 0$ when z_2 is a ‘clean’ signal, $w = 0$. In the presence of noise, $w \neq 0$, it occurs that R is slightly greater than zero. The detection is then completed based on a specified (small) threshold γ , $\gamma > 0$, being obviously that the greater is the power of the noise the greater should be γ .

As a matter of convenience the algorithm is summarized below:

4.1 Algorithm of the New Chaos Detector

- 1) consider an observation window of N points and initialize it with zeros;
- 2) initialize the ratio R with zero, $R(0) = 0$;

- 3) get $y_{obs}(n)$ with a specified sampling period dt ; $n = 1, 2, \dots$
- 4) solve $\dot{z} = Az + by_{obs}$ step-by-step with a step size = dt ;
- 5) if $z_2(n)$ is a local maximum
 - update the observation window with the respective $\arg \max t_n$;
 - calculate the Δt 's between the local maxima, $\Delta t_n = t_{n+1} - t_n$;
 - sort the Δt 's in ascending order λ ;
 - calculate the $\Delta(\Delta t)$'s, $\Delta(\Delta t)_n = \Delta t_{n+1} - \Delta t_n$;
 - discard the points whose values immediately before and after are both zero;
 - compute the ratio $R(n)$;
- else
 - keep the previous ratio, $R(n) = R(n - 1)$;
- end
- 6) if $R(n) > \gamma$, with $\gamma > 0$
 - “chaotic behaviour”
 - $R_{bi-state}(n) = true$
- else
 - “regular behaviour”
 - $R_{bi-state}(n) = false$
- end
- 7) go indefinitely to step (3);

Note that the proposed algorithm is always feasible unless the running time between steps (3) and (6), ΔT , exceeds the elapsed time between successive measurements, $y_{obs}(n)$, $n = 1, 2, \dots$, that is, the sampling period, defined by dt . This way, $\Delta T < dt$ is the unique feasibility condition to allow a real-time detection. Another remark that is worth mentioning can be found in step (5). Given the need of finding the local maxima of z_2 , the algorithm must be applied considering a delay of one measurement $y_{obs}(n)$ because it is needed three points to determine whether the midpoint is a local maximum or not. Nevertheless, this is not problematic since a single point has no effect when deciding the type of behaviour.

In the absence of noise, $w = 0$, the idea behind the detector could be applied directly to an observation window containing the time-instants t_1, \dots, t_N for which y_{obs} exhibits local maxima. Nevertheless, when y_{obs} is corrupted with noise, $w \neq 0$, the method would be no longer effective because WGN has random maxima at random samples. The obvious thought would be the introduction of noise-

reduction techniques such as Kalman filters since they are applicable in real-time. However, that solution would not ensure a successful detection because the underlying dynamics of chaotic systems is not localized either in the time or in the frequency domain. That is why equation (2) plays an important role. Being a linear system and A a stable matrix, z_2 has not necessarily the waveform of y_{obs} but inherits its essential dynamics, acting therefore as a ‘noise reducer’. A noisy signal y_{obs} with a specified SNR produces a noisy signal z_2 with a SNR substantially lower. Otherwise, the signal directly under analysis, y_{obs} , would exhibit an ‘infinite’ number - very large, depending on the size of the observation window - of local maxima due to the presence of noise, and chaos would be confused with a purely stochastic signal.

5 Simulation Results

This section deals with the validation of the proposed detector. Numerical simulations are carried out for three applications: a butterfly-shaped system similar to the well-known Lorenz system; and two aerospace systems - the attitude motion of a magnetic rigid spacecraft in an elliptical orbit, and the attitude motion of an electro-mechanical gyrostat. The transition between the regular to the chaotic behaviour occurs through a change of the system parameters, representing possible parameter uncertainties. White Gaussian Noise is added to the observable outputs to prove the robustness of the detector.

5.1 Application 1: Butterfly-Shaped System

Consider a three-dimensional, continuous-time, time-invariant nonlinear system with dynamics described by the following differential equations, [50]:

$$\begin{aligned}\dot{x}_1 &= a(x_2 - x_1 + x_2x_3) \\ \dot{x}_2 &= bx_2 - hx_1x_3 \\ \dot{x}_3 &= kx_2 - gx_3\end{aligned}\quad (4)$$

wherein x_1, x_2, x_3 denote the system state variables and a, b, h, k, g the system parameters. System (4) exhibits periodic-, quasi-periodic-, or chaotic-trajectories, depending on the values of the parameters. For $a = h = k = 1.0$, $b = 2.5$, and $g = 3.9$, the system exhibits a transverse butterfly-shaped attractor similar to the well-known Lorenz attractor as depicted in Fig. 3. Increasing g

continuously within the interval $g \in [3.0, 4.0]$ and keeping all the other parameters unchanged, occurs a successive period-doubling that leads a regular- to a chaotic- behaviour as shows the bifurcation diagram of the first state variable, x_1 , see Fig. 4:

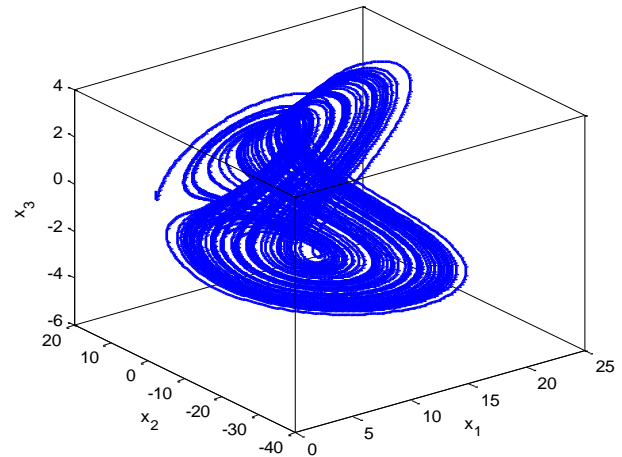


Fig. 3. Chaotic attractor for $g = 3.9$.

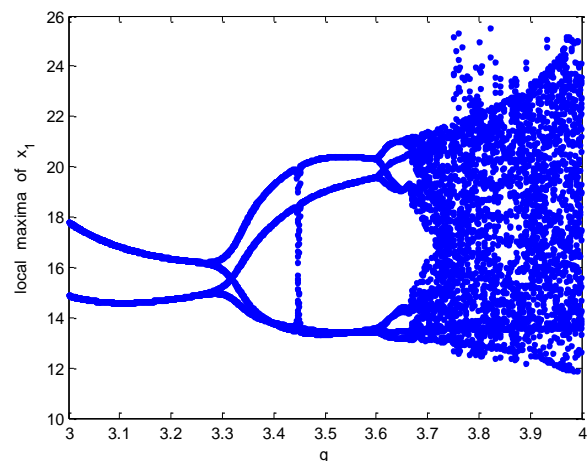


Fig. 4. Bifurcation diagram of the variable x_1 .

5.1.1 Simulation

For simulation purposes, equations (4) were solved through the RK-Butcher method between $t_0 = 0$ and $t_f = 1000$ s, with a step of $\delta t = 0.005$ s, and departing from initial conditions $x_0 = [x_1, x_2, x_3]_0^T = [1, 1, 1]^T$. The first state variable, x_1 , is taken as the observable output, and it is based on it that the detector classifies the type of motion. The ‘measurements’, $y_{obs}(n) = x_1(n) + w(n)$, are carried out with a sampling period of $dt = 0.01$ s considering a Signal-to-Noise Ratio of $SNR = 14$ dB, that is, a relationship of 5:1. The observation window has length $N = 50$ points and equation \dot{z} the following form:

$$\begin{bmatrix} \dot{z}_1 \\ \dot{z}_2 \end{bmatrix} = \begin{bmatrix} -0.5 & 0 \\ 1 & -0.5 \end{bmatrix} \begin{bmatrix} z_1 \\ z_2 \end{bmatrix} + \begin{bmatrix} 1 \\ 0 \end{bmatrix} y_{obs}, \quad z_0 = \begin{bmatrix} 0 \\ 0 \end{bmatrix} \quad (5)$$

where A is a stable matrix with eigenvalues $\lambda = (-0.5, -0.5)$. The threshold between the regular- and the chaotic- behaviour was set in $\gamma = 5$.

Fig. 5 shows the results. The first plot represents the variation over the time of parameter g - the parameter used to trigger different types of behaviour; the second plot represents the output of the system, $y = x_1$; the third plot the measured signal, $y_{obs}(n) = x_1(n) + w(n)$; and the last plot the output of the detector: R given by equation (3); and R bi-state indicating a chaotic or a non-chaotic behaviour based on the threshold γ .

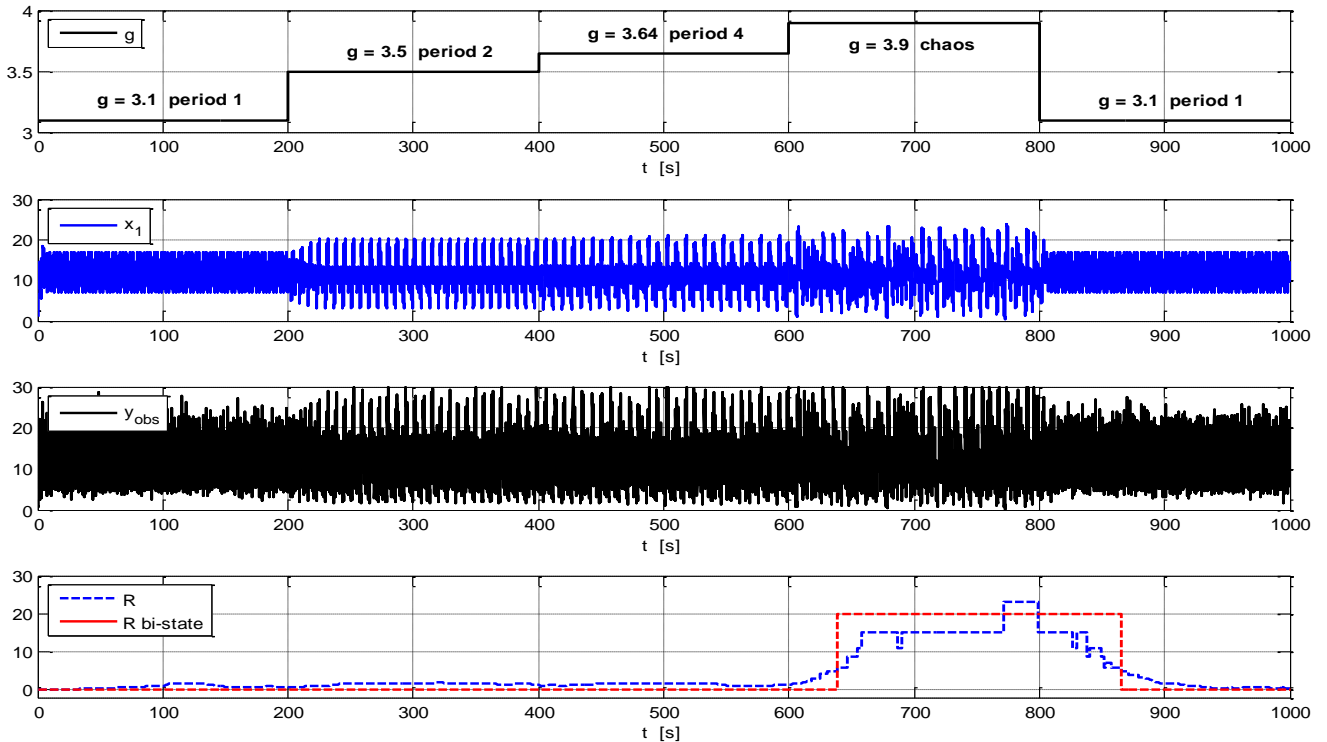


Fig. 5. Chaos detection in the butterfly-shaped system.

5.2 Application 2: Attitude Motion of a Magnetic Rigid Spacecraft in an Elliptical Orbit

The attitude motion of an uncontrolled magnetic rigid spacecraft, with internal damping, moving in an elliptical orbit subject to both gravitational and magnetic fields of the Earth, is given by equations, [51], [52]:

$$\begin{aligned} \frac{dx_1}{dv} &= x_2 \\ \frac{dx_2}{dv} &= \frac{2e \sin x_3}{1 + e \cos x_3} (1 + x_2) - \frac{\kappa \sin 2x_1}{1 + e \cos x_3} + \dots \\ &\quad \dots - \frac{\gamma}{(1 + e \cos x_3)^2} x_2 + \dots \\ &\quad \dots + \alpha \frac{3 \cos(x_1 - x_3 - \omega) - \cos(x_1 + x_3 + \omega)}{1 + e \cos x_3} \end{aligned}$$

$$\frac{dx_3}{dv} = 1 \quad (6)$$

where $x_1 = \phi$, $x_2 = d\phi/dv$, $x_3 = v$, in which ϕ denotes the libration angle in the orbital plane, v the true anomaly of the spacecraft, that is, the angle between the perigee and the vehicle, measured in the plane of the orbit, ω the argument of perigee, that is, the angle between the ascending node and the perigee, e the orbital eccentricity, κ a parameter related to the principal moments of inertia, that describes therefore the spacecraft's asymmetry, γ the damping coefficient, and α a magnetic parameter describing the strength of the magnetic interaction between the Earth's magnetic field and the magnetic moment of the spacecraft. The angles v, ϕ, ω are expressed in rad.

System (6) exhibits a regular behaviour for the values of parameters presented in (i) and a chaotic behaviour for the parameters in (ii). A tiny variation in the magnetic parameter, $\delta\alpha = 0.001$, is enough to trigger an unpredictable motion, which is one of the main characteristics of chaotic systems: high sensitivity to parameter changes. The phase-spaces, or more precisely the phase-planes $x_1 - x_2$ because the original system is ‘time’-varying and there is no interest in representing the third variable x_3 , are depicted in Figs. 6 and 7 respectively for the condition of regular/periodic- and chaotic- motion.

(i) $e = 0.2, \kappa = 1.0, \gamma = 0.1, \omega = 60.\pi/180,$
 $\alpha = 0.336$ (regular behaviour)

(ii) $e = 0.2, \kappa = 1.0, \gamma = 0.1, \omega = 60.\pi/180,$
 $\alpha = 0.337$ (chaotic behaviour)

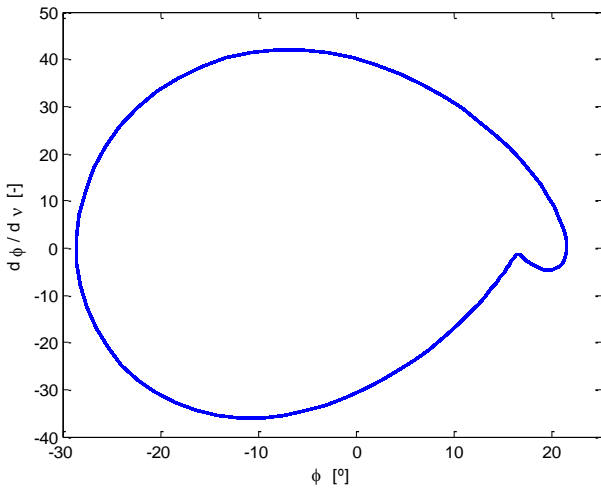


Fig. 6. Periodic motion for $\alpha = 0.336$.

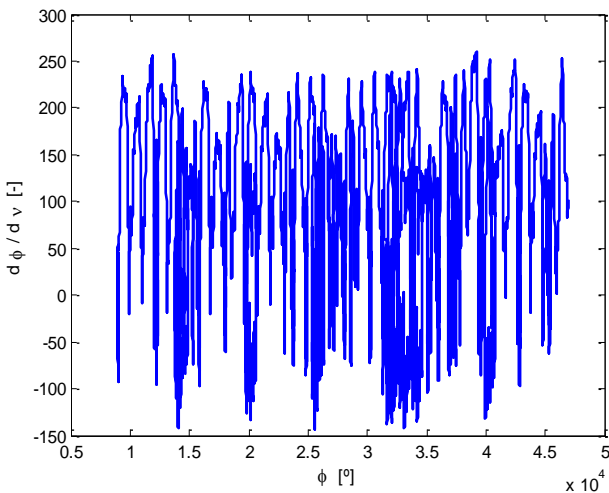


Fig. 7. Chaotic motion for $\alpha = 0.337$.

5.2.1 Simulation

For this application, equations (6) were solved through the RK-Butcher method between $\nu_0 = 0$ and $\nu_f = 2\pi.1000$ rad (the spacecraft travels 1000 laps in the orbital plane), with a step of $\delta\nu = 2\pi/200$ rad, and departing from initial conditions $x_0 = [\phi, d\phi/d\nu, \nu]_0^T = [0, 0, 0]^T$. The observable output taken into consideration is the second state variable, $x_2 = d\phi/d\nu$, the ‘measurements’, $y_{obs}(n) = x_2(n) + w(n)$, are performed with a sampling rate of $d\nu = 2\pi/100$ rad, and the level of noise is $SNR = 10$ dB ($\cong 3:1$). The observation window has length $N = 50$ points and equation \dot{z} the following form:

$$\begin{bmatrix} \dot{z}_1 \\ \dot{z}_2 \end{bmatrix} = \begin{bmatrix} -1 & 0 \\ 1 & -1 \end{bmatrix} \begin{bmatrix} z_1 \\ z_2 \end{bmatrix} + \begin{bmatrix} 1 \\ 0 \end{bmatrix} y_{obs} \quad , \quad z_0 = \begin{bmatrix} 0 \\ 0 \end{bmatrix} \tag{7}$$

where A is a stable matrix with eigenvalues $\lambda = (-1, -1)$. The threshold between the regular- and the chaotic- behaviour was set in $\gamma = 1$.

Fig. 8 shows the results. The first plot represents the variation of the magnetic parameter, α , along the position of the spacecraft in its orbit - the parameter used to toggle between the regular- and the chaotic- behaviour; the second plot represents the output of the system, $y = d\phi/d\nu$; the third the measured signal, $y_{obs}(n) = d\phi/d\nu(n) + w(n)$; and the last plot the output of the detector: R given by equation (3); and R bi-state indicating a chaotic- or a non-chaotic- behaviour based on the threshold γ .

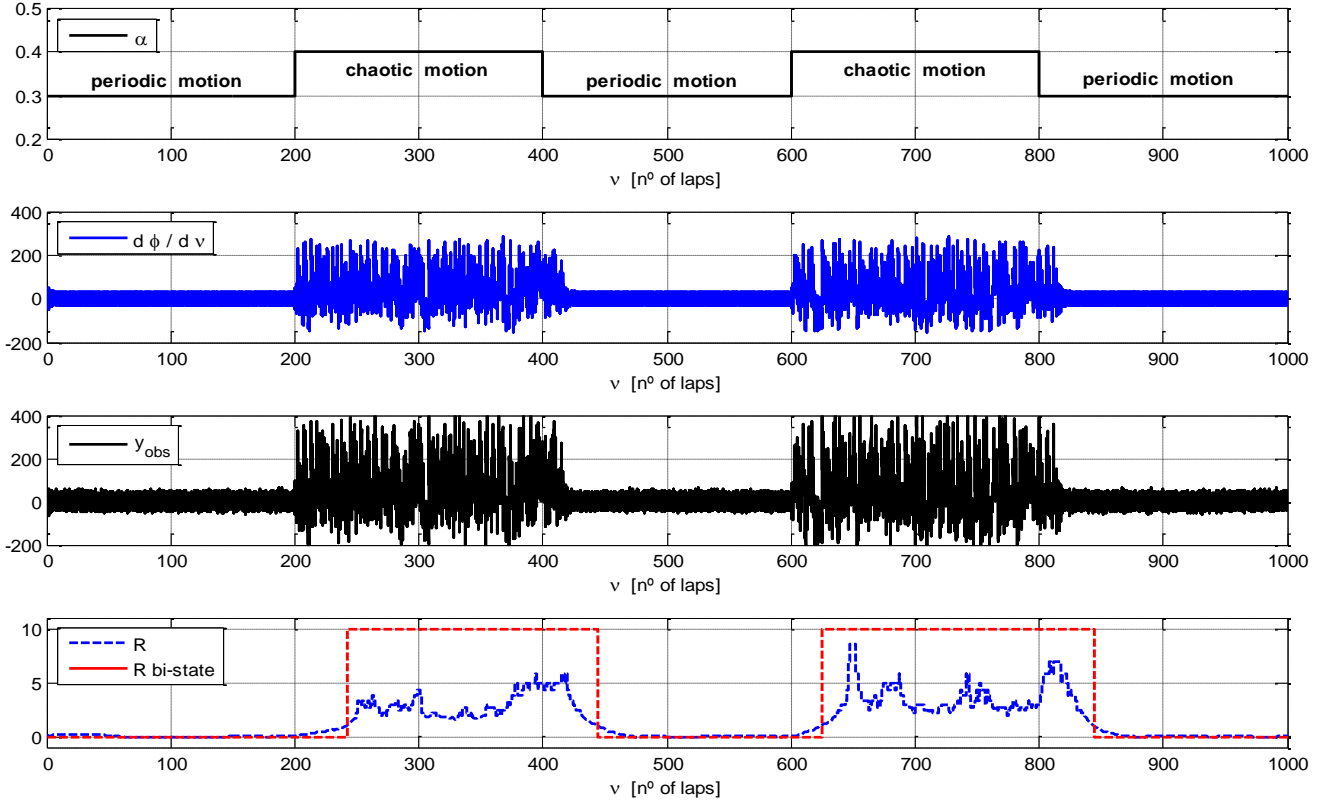


Fig. 8. Chaos detection in the attitude motion of a magnetic rigid spacecraft in an elliptical orbit.

5.3 Application 3: Dynamics of an Electro-Mechanical Gyrostat

An electro-mechanical gyrostat is a fourth-order, time-varying, nonlinear system with great interest in the aerospace field. It consists of three rotors orthogonal to each other aligned with the principal axes of inertia of the body (e.g.: satellite, spacecraft, etc.), that allow the control of the attitude motion by varying the torque produced by a control-motor. The dynamical model of an electro-mechanical gyrostat can be expressed as, [53], [54]:

$$\dot{x} = (A + A_1(t))x + \varphi(x, t) \quad (8)$$

with:

$$A = \begin{bmatrix} -k_1/I_1 & -h_3/I_1 & h_2/I_1 & 0 \\ h_3/I_2 & -k_3/I_2 & -h_1/I_2 & 0 \\ -h_2/I_3 & h_1/I_3 & -(b + k_5)/I_3 & K_T/I_3 \\ 0 & 0 & -(K_a + K_b)/L & -R/L \end{bmatrix}$$

$$A_1(t) = \begin{bmatrix} 0 & -h_3/I_1 \cdot f \cos(\omega t) & 0 & 0 \\ h_3/I_2 \cdot f \cos(\omega t) & 0 & 0 & 0 \\ 0 & 0 & 0 & 0 \\ 0 & 0 & 0 & 0 \end{bmatrix}$$

$$\varphi(x, t) = \begin{bmatrix} (I_2 - I_3)/I_1 \cdot x_2 x_3 \\ (I_3 - I_1)/I_2 \cdot x_1 x_3 \\ (I_1 - I_2)/I_3 \cdot x_1 x_2 + k_6/I_3 \cdot (\omega_r^3 - x_3^3) \\ K_a/L \cdot \omega_r \end{bmatrix} + \eta$$

$$\eta = \begin{bmatrix} k_2/I_1 \cdot (\omega_r^3 - x_1^3) + k_1/I_1 \cdot \omega_r \\ k_4/I_2 \cdot (\omega_r^3 - x_2^3) + k_3/I_2 \cdot \omega_r \\ k_5/I_3 \cdot \omega_r + h_3/I_3 \cdot f \omega \sin(\omega t) \\ 0 \end{bmatrix} \quad (9)$$

with $x = [x_1, x_2, x_3, x_4]^T = [\omega_x, \omega_y, \omega_z, i]^T$, where $\omega_x, \omega_y, \omega_z$ denote the angular velocities of the gyrostat on the axes x, y, z , respectively, and i the electric current of the control-motor. I_1, I_2, I_3 represent the principal moments of inertia of the gyrostat, h_1, h_2, h_3 the angular moments of the rotors - located on the axes x, y, z , respectively, ω_r the projection of the angular velocity of the gyrostat on the axes x, y, z for which it was designed, and b the damping coefficient. K_T, L, R denote respectively the torque constant, the inductance and the resistance of the control-motor. K_a, K_b are two parameters related respectively to the electromotive and counter-electromotive forces of the control-motor. The angular moment of the third rotor, h_3 , is subject to a time-periodic disturbance of the form $h_3 \cdot f \cos(\omega t)$, so that f and ω denote respectively

the magnitude and the excitation frequency. The angular velocities $\omega_x, \omega_y, \omega_z$ are expressed in rad/s and the electric current i in A.

System (8) exhibits a regular behaviour for the values of parameters presented below along with condition (i), and a chaotic behaviour with condition (ii). A variation in the magnitude of the disturbance of h_3 is sufficient to trigger a chaotic dynamics. The respective phase-spaces, or, specifically, the phase-planes with variables $x_4 - x_1 - x_2$, are shown in Figs. 9 and 10.

$$I_1 = I_2 = 500, I_3 = 1000, h_1 = h_2 = 200, h_3 = 250, k_i = 1 (i = 1, \dots, 6), K_T = 300, K_a = 50, K_b = 1.3, L = 2, R = 100, \omega_r = 0, \omega = 1, b = 200$$

- (i) $f = 13.6$ (regular behaviour)
- (ii) $f = 12.9$ (chaotic behaviour)

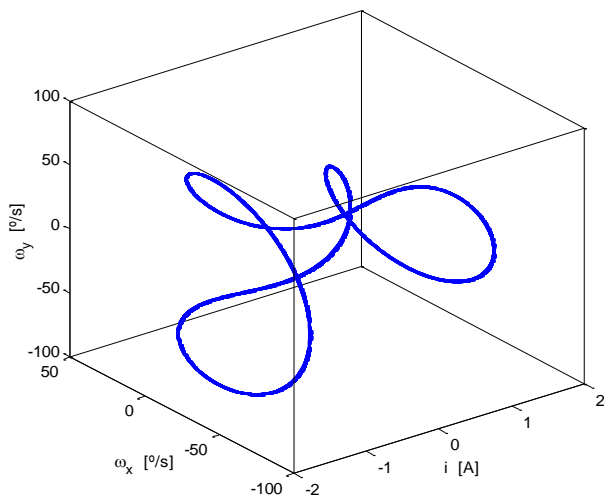


Fig. 9. Periodic motion for $f = 13.6$.

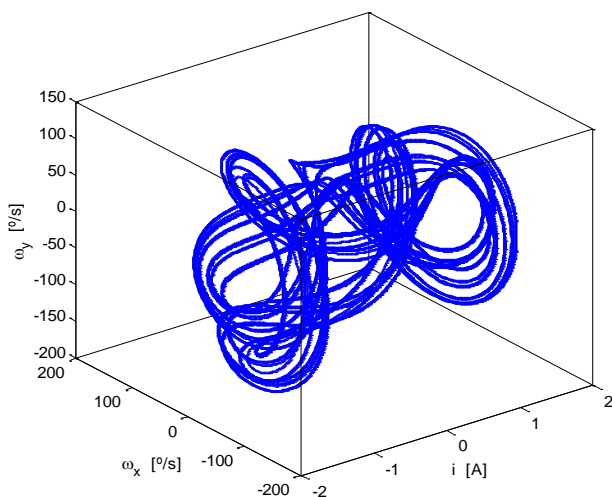


Fig. 10. Chaotic motion for $f = 12.9$.

5.3.1 Simulation

In this application, equation (8) was solved through the RK-Butcher method for time-varying systems, between $t_0 = 0$ and $t_f = 1800$ s, with a step of $\delta t = 0.01$ s, and departing from initial condition $x_0 = [\omega_x, \omega_y, \omega_z, i]_0^T = [0, 0, 0, 0]^T$. The observable output taken into consideration is the first state variable, $x_1 = \omega_x$, the ‘measurements’, $y_{obs}(n) = x_1(n) + w(n)$, are performed with a sampling period of $dt = 0.01$ s, and the level of signal degradation with WGN is SNR = 10 dB ($\cong 3:1$). The observation window has length $N = 50$ points and equation \dot{z} the following form:

$$\begin{bmatrix} \dot{z}_1 \\ \dot{z}_2 \end{bmatrix} = \begin{bmatrix} -1 & 0 \\ 1 & -1 \end{bmatrix} \begin{bmatrix} z_1 \\ z_2 \end{bmatrix} + \begin{bmatrix} 1 \\ 0 \end{bmatrix} y_{obs} \quad , \quad z_0 = \begin{bmatrix} 0 \\ 0 \end{bmatrix} \tag{10}$$

where A is a stable matrix with eigenvalues $\lambda = (-1, -1)$, and the threshold was set in $\gamma = 1$.

Fig. 11 shows the results after discarding the initial transient regime (300 s). The first plot represents the variation over the time of the parameter f - the parameter used to toggle between the regular- and the chaotic- behaviour; the second plot represents the output of the system, $y = \omega_x$; the third plot the measured signal, $y_{obs}(n) = \omega_x(n) + w(n)$; and the last plot the output of the detector: R given by equation (3); and R bi-state indicating a chaotic- or a non-chaotic- behaviour based on the threshold γ .

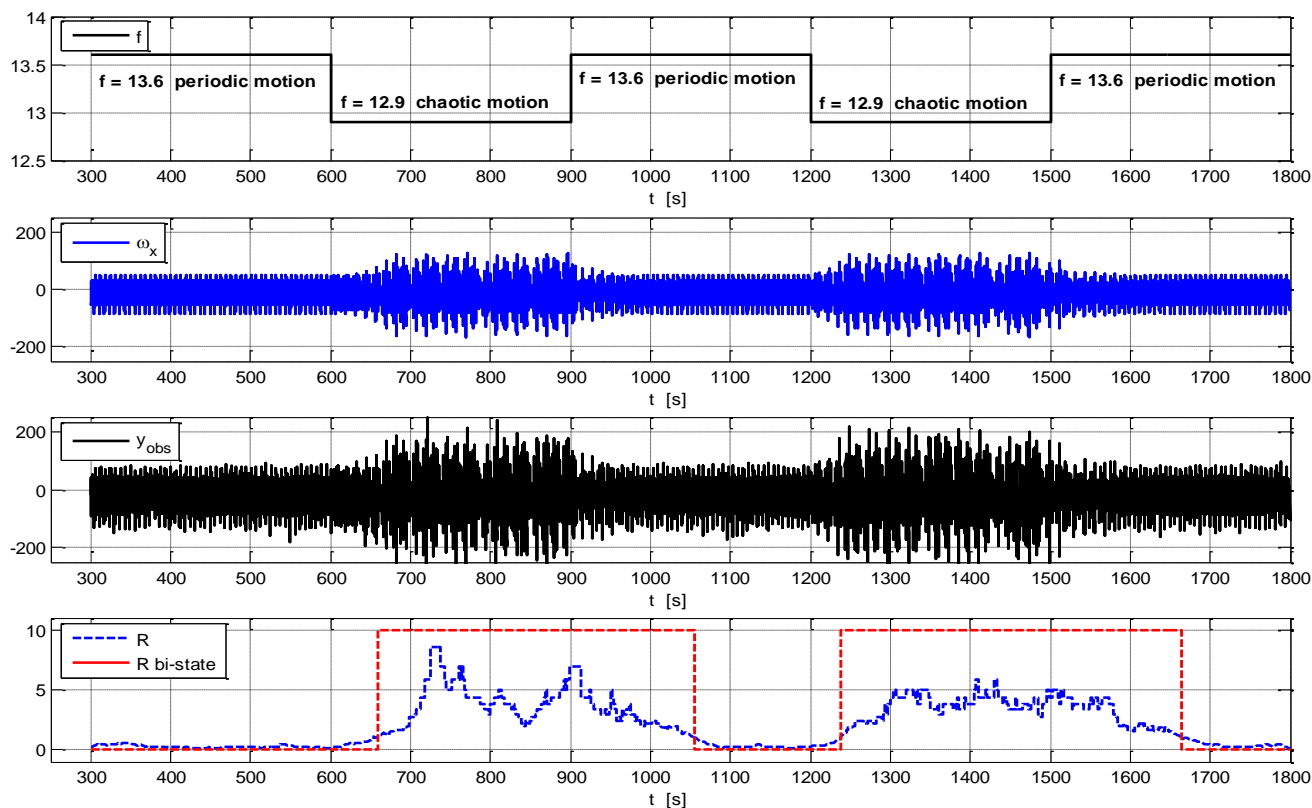


Fig. 11. Chaos detection in the dynamics of an electro-mechanical gyrostator.

6 Discussion

The results show that the chaotic dynamics is effectively detected in all three applications, from a single time series, and corrupted with WGN. Obviously, there is a small delay between each transition - from the regular- to the chaotic-behaviour, and vice versa - see Figs. 5, 8, 11, but which is perfectly normal since, like any other detection method, a representative sample of the signal is required to characterize the type of motion. As is intuitive, the greater is the length of the observation window N , the greater is the delay of the detection, and in that sense the proposed detector works very well with a short window of only $N = 50$ points, regardless of a slow or a fast dynamics. Conversely, as the power of the noise increases, that is, for lowers $\text{SNR}_{\text{dB}} = 20 \log(A_s/\sigma_n)$, greater must be the observation window to counteract the effects of noise. There is therefore a compromise between the length of the observation window N , the SNR of the measured signal y_{obs} , and the delay of the detection. Even so, recall that there is always a transient regime between each transition, where the motion is neither regular nor chaotic, and therefore the delays observed in Figs. 5, 8, 11 can be considered as being really short.

Another worth mentioning point is related to the value of R . According to the description of the algorithm, where for a 'clean' signal ($w = 0$), $R = 0$ specifies a regular behaviour and $R \gg 0$ a chaotic behaviour, it is evident that the more chaotic is the signal y_{obs} , the greater is the value of R , and the same applies to a corrupted signal ($w \neq 0$). Despite not being presented here because it is not of great relevance for the present paper, simulations were also performed using as inputs the signal of a chaotic attractor (3D Rössler system, [55]) and the signal of a hyperchaotic attractor (4D Rössler system, [56]) to verify that R is indeed greater.

The results show also that the distinction between the regular- and the chaotic- behaviour is extremely clear. As depicted in Fig. 5, a chaotic behaviour, $R > \gamma$, is indicated only and only when the measured signal, y_{obs} , is in fact chaotic. The transitions between different periodic behaviours (period 1 \rightarrow period 2 \rightarrow period 4) are identified as being regular behaviours, $R \leq \gamma$, as desired. Unsurprisingly, there is a slight change in the value of R but which is obviously not enough to reach the specified threshold γ given the number of points of the observation window.

With respect to the value of the threshold γ , one knows that, for a ‘clean’ signal y_{obs} , the value of R is practically zero in case of a regular input and much greater than zero in case of a chaotic input; $R \approx 0$ and $R \gg 0$, respectively; so that the threshold can be set, for example, in $\gamma = 0.1$. Nevertheless, as the SNR decreases, the threshold γ should be increased to overcome the effects induced by the presence of noise. According to simulations performed, a threshold of $\gamma = 1$ is an appropriate choice and provides excellent results for relatively low SNR’s.

The unique point of the proposed algorithm that may require a special attention is the measurement sampling frequency $f_s = 1/dt$. If f_s is too low, the Δt ’s sorted in ascending order (stairs of Fig. 2) appear in large number, indicating erroneously the presence of a chaotic motion when actually may be a (quasi)periodic motion. Hence, a proper selection of the sampling frequency is required to ensure that the essential dynamic of the measured signal y_{obs} is captured. Unsurprisingly, this was already expected and can be seen actually as an advantage of the detector. Notice that, the higher is the sampling frequency f_s , better is the detection in the sense that R approaches even more (or moves away) from zero, and this way one not need to worry about possible oversampling as opposed to other detection techniques.

6.1 Computational Complexity Analysis

Since one of the main objectives of the proposed detector is the detection in real-time of chaotic modes, it becomes interesting to evaluate its complexity in computational terms. To achieve this, the complexity of the algorithm is compared with the complexity of the *0-1 Test*, formulated by [2] - a test, say, in the same condition, in the sense that chaos can be detected from a single time series. Following reference [57], the computational complexity of a given algorithm is theorized by the ratio: $L_i = T_i/T_0$, where T_i denotes the average running time of the algorithm i , and T_0 the average running time of a *Test Code* composed by a set of simple operations:

Test Code:

```
x = 5.55; (double)
for i = 1:1000000
    x = x + x;    x = x * x;    x = x / 2;
    x = sqrt(x); x = exp(x); x = ln(x);
end
```

Using this definition, the *0-1 Test* (with $c \in [\pi/5, 4\pi/5]$, $N_c = 100$ and K computed by the correlation method, see [5] for details) and the algorithm presented in this paper have complexities respectively of $L_1 \cong 3.2$ and $L_2 \cong 1.3 \times 10^{-3}$, corresponding respectively to the average running times $T_1 \cong 498$ ms and $T_2 \cong 0.203$ ms and to an average running time of the *Test Code* on the computer used for this purpose of $T_0 \cong 154$ ms. The signal under analysis was a time series of length $N = 1000$ points obtained by discretization, with sampling frequency $f_s = 10$ Hz ($dt = 0.1$ s), of the first variable of system (4), x_1 , and the average running times T_0, T_1, T_2 were calculated running each algorithm 100 times. When compared to the *0-1 Test*, the proposed detector clearly requires a low computational effort. This is due to the fact that while the *0-1 Test* requires the computation of several integrals and multiplications to obtain a transformed input signal, the proposed algorithm requires only the computation of simple operations given that equation (2) can be solved as a new measurement is available.

7 Concluding Remarks

In the present paper a new algorithm for chaos detection in real-time, automatically, from a single time series and in the presence of noise, is proposed. The principle of detection is based on one of the main characteristics of chaotic systems: any trajectory, regardless of its initial condition, becomes highly unpredictable after a very short period of time. It occurs then that a single component of the trajectory - the measured signal - is a random-like motion that exhibits ‘infinite’ local maxima at different time-instants. It is then established a sliding observation window comprising such time-instants, and after a simple data manipulation a parameter, R , specifies between two types of dynamics: a regular motion (equilibrium state, periodic, multi-periodic); or a chaotic motion. The decision process is based on a specified threshold γ : $R \leq \gamma$ indicates a regular motion; and $R > \gamma$ a chaotic motion.

Numerical simulations are performed to validate the effectiveness of the detector using three applications: a butterfly-shaped system similar to well-known Lorenz system; the attitude motion of a magnetic rigid spacecraft in an elliptical orbit; and the attitude motion of an electro-mechanical gyrostat; and in all of them it is taken into account White Gaussian Noise (WGN) to evaluate the robustness of the detector. The results show that the

distinction is very clear. A chaotic behaviour is identified when and only when the underlying dynamics is actually chaotic, and not when it occurs for example a simple change of behaviour, such as a variation in the oscillation frequency or a bifurcation. Moreover, the detection is successfully achieved for levels of signal degradation in the order of $\text{SNR} = 10$ dB (a ratio between the signal and noise of $\cong 3:1$, respectively) which is more than enough for most engineering applications.

The most powerful aspects of the proposed detector is that it does not require the system model neither estimation of all the state variables, or the reconstruction of the phase-space, that is, knowledge of the full trajectory, because the detection is independent of the nature of the data. The algorithm is simply applied to a unique time series, and because of that there is no restriction about the dimension of the system. Another advantage is related to the length of the observation window. The detection is effective even for a very small observation window of only 50 points. In addition, since the detector is based on the local maxima, there is no need of worrying about the sampling frequency regardless of a fast or slow dynamics, as opposed to other techniques that require a special attention to avoid oversampling phenomena. Lastly, the low complexity of the algorithm is another great advantage which makes it definitely appropriate for detection in real-time. It is very efficient from the computational point of view, both in terms of programming efforts as in terms of actual computation time.

As a future work, it would be interesting to carry out a thorough study to find out the possibility of establishing a relationship between the level of noise - assuming that it is known - and the threshold γ , in order to improve (decrease) the SNR of the detector. Note that the introduction of a non-linear filter would certainly bring benefits. However, this is not so straightforward and requires developing new real-time noise reduction techniques since the conventional ones are not appropriate for chaotic dynamics (see [58], [59] for details). With respect to the complexity of the detector, it would be also interesting to carry out a formal analysis about the computational complexity and compare it to other algorithms. Another idea, which is actually being prepared by the same authors, is an extension of the proposed concept of detection for discrete-time systems (maps).

Acknowledgments:

This research was conducted in the Aeronautics and Astronautics Research Unit of the University of Beira Interior (LAETA - UBI / AeroG) at Covilhã, Portugal, and supported by the Portuguese Foundation for Science and Technology (FCT) through the following funding program:



References:

- [1] J. S. A. E. Fouda, J. Y. Effa, M. Kom, and M. Ali, The Three-state Test for Chaos Detection in Discrete Maps, *Applied Soft Computing*, Vol. 13, No. 12, 2013, pp. 4731–4737.
- [2] G. A. Gottwald and I. Melbourne, A New Test for Chaos in Deterministic Systems, *Proceedings of the Royal Society A: Mathematical, Physical & Engineering Sciences*, Vol. 460, No. 2042, 2004, pp. 603–611.
- [3] P. V. McDonough, J. P. Noonan, and G. R. Hall, A New Chaos Detector, *Computers & Electrical Engineering*, Vol. 21, No. 6, 1995, pp. 417–431.
- [4] I. Djurović, V. Rubežić, and E. Sejdić, A Scaling Exponent-based Detector of Chaos in Oscillatory Circuits, *Physica D: Nonlinear Phenomena*, Vol. 242, No. 1, 2013, pp. 67–73.
- [5] G. A. Gottwald and I. Melbourne, On the Implementation of the 0-1 Test for Chaos, *SIAM Journal on Applied Dynamical Systems*, Vol. 8, No. 1, 2009, pp. 129–145.
- [6] C. S. Poon and M. Barahona, Titration of Chaos with Added Noise, *Proceedings of the National Academy of Sciences of the United States of America*, Vol. 98, No. 13, 2001, pp. 7107–7112.
- [7] J. Awrejcewicz and L. Dzyubak, Quantifying Smooth and Nonsmooth Regular and Chaotic Dynamics, *International Journal of Bifurcation and Chaos*, Vol. 15, No. 6, 2005, pp. 2041–2055.
- [8] J. Awrejcewicz, L. Dzyubak, and C. Grebogi, A Direct Numerical Method for Quantifying Regular and Chaotic Orbits, *Chaos, Solitons & Fractals*, Vol. 19, No. 3, 2004, pp. 503–507.

- [9] H. G. Schuster, *Handbook of Chaos Control*, 1st ed., Weinheim: WILEY-VCH Verlag GmbH, 1999.
- [10] W. Ditto and T. Munakata, Principles and Applications of Chaotic Systems, *Communications of the ACM*, Vol. 38, No. 11, 1995, pp. 96–102.
- [11] E. Ott and M. Spano, Controlling Chaos, *Chaotic, Fractal, and Nonlinear Signal Processing. AIP Conference Proceedings*, Vol. 375, 1995, pp. 92–103.
- [12] K. Bousson and C. M. N. Velosa, Robust Control and Synchronization of Chaotic Systems with Actuator Constraints, in *Handbook of Research on Artificial Intelligence Techniques and Algorithms*, P. Vasant, Ed. IGI Global, 2015, pp. 1–43.
- [13] G. Cheng and Y. Z. Liu, Chaotic Motion of a Magnetic Rigid Satellite in an Orbit near the Equatorial Plane of the Earth, *Journal "Technische Mechanik"*, Vol. 19, No. 2, 1999, pp. 197–201.
- [14] C. M. N. Velosa and K. Bousson, Synchronization of Chaotic Systems with Bounded Controls, *International Review of Automatic Control (IREACO)*, (To appear).
- [15] C. M. N. Velosa and K. Bousson, Suppression of Chaotic Modes in Spacecraft with Asymmetric Actuator Constraints, *Proceedings of the Institution of Mechanical Engineers, Part G: Journal of Aerospace Engineering*, (To appear).
- [16] C. M. N. Velosa and K. Bousson, Robust Output Regulation of Uncertain Chaotic Systems with Input Magnitude and Rate Constraints, *Acta Mechanica et Automatica*, (To appear).
- [17] E. Ott, C. Grebogi, and J. A. Yorke, Controlling Chaos, *Physical Review Letters*, Vol. 64, No. 11, 1990, pp. 1196–1199.
- [18] K. Pyragas, Continuous Control of Chaos by Self-Controlling Feedback, *Physics Letters A*, Vol. 170, No. 6, 1992, pp. 421–428.
- [19] L. M. Pecora and T. L. Carroll, Synchronization in Chaotic Systems, *Physical Review Letters*, Vol. 64, No. 8, 1990, pp. 821–824.
- [20] M. Otani and A. J. Jones, Guiding Chaotic Orbits: Research Report, 1997.
- [21] K. Bousson, Synchronization of a Chaotic Gyroscopic System under Settling Time Constraints, *Journal of Vibroengineering*, Vol. 14, No. 3, 2012, pp. 1299–1305.
- [22] C. Ki Ahn, $L_2 - L_\infty$ Chaos Synchronization, *Progress of Theoretical Physics*, Vol. 123, No. 3, 2010, pp. 421–430.
- [23] F. C. Moon, *Chaotic and Fractal Dynamics: An Introduction for Applied Scientists and Engineers*, 1st ed., Birkach: WILEY-VCH Verlag GmbH & Co. KGaA, 1992.
- [24] S. Boccaletti, C. Grebogi, Y. C. Lai, H. Mancini, and D. Maza, The Control of Chaos: Theory and Applications, *Physics Reports*, Vol. 329, No. 3, 2000, pp. 103–197.
- [25] E. N. Lorenz, *The Essence of Chaos*. London: UCL Press Limited, University College London, 1995.
- [26] G. C., E. Ott, S. Pelikan, and J. A. Yorke, Strange Attractors that are not Chaotic, *Physica D: Nonlinear Phenomena*, Vol. 13, No. 1–2, 1984, pp. 261–268.
- [27] Z. Zhu and Z. Liu, Strange Nonchaotic Attractors of Chua's Circuit with Quasiperiodic Excitation, *International Journal of Bifurcation and Chaos*, Vol. 07, No. 01, 1997, pp. 227–238.
- [28] E. Ott, *Chaos in Dynamical Systems*, 1st ed., Cambridge University Press, 1993.
- [29] M. Gidea and C. P. Niculescu, *Chaotic Dynamical Systems: An Introduction*. Craiova; Universitaria Press, 2002.
- [30] A. H. Nayfeh and B. Balachandran, *Applied Nonlinear Dynamics: Analytical, Computational, and Experimental Methods*, 1st ed., John Wiley & Sons, 1995.
- [31] M. Marek and I. Schreiber, *Chaotic Behaviour of Deterministic Dissipative Systems*. Cambridge University Press, 1995.
- [32] A. Wolf, J. B. Swift, H. L. Swinney, and J. A. Vastano, Determining Lyapunov Exponents from a Time Series, *Physica D: Nonlinear Phenomena*, Vol. 16, No. 3, 1985, pp. 285–317.
- [33] H. Kantz and T. Schreiber, *Nonlinear Time Series Analysis*, 2nd ed., Cambridge University Press, 2004.
- [34] M. Sano and Y. Sawada, Measurement of the Lyapunov Spectrum from a Chaotic Time Series, *Physical Review Letters*, Vol. 55, No. 10, 1985, pp. 1082–1085.
- [35] J.-P. Eckmann, S. O. Kamphorst, D. Ruelle, and S. Ciiliberto, Lyapunov Exponents from Time Series, *Physical Review A*, Vol. 34, No. 6, 1986, pp. 4971–4979.
- [36] R. Brown, P. Bryant, and H. D. I. Abarbanel, Computing the Lyapunov Spectrum of a Dynamical System from a Observed Time

- Series, *Physical Review A*, Vol. 43, No. 6, 1991, pp. 2787–2806.
- [37] M. T. Rosenstein, J. J. Collins, and C. J. De Luca, A Practical Method for Calculating Largest Lyapunov Exponents from Small Data Sets, *Physica D: Nonlinear Phenomena*, Vol. 65, No. 1–2, 1993, pp. 117–134.
- [38] H. Kantz, A Robust Method to Estimate the Maximal Lyapunov Exponent of a Time Series, *Physics Letters A*, Vol. 185, No. 1, 1994, pp. 77–87.
- [39] V. K. Melnikov, On the Stability of the Center for Time-Periodic Perturbations, *Transactions of the Moscow Mathematical Society*, Vol. 12, 1963, pp. 1–57.
- [40] L. Perko, *Differential Equations and Dynamical Systems*, 3rd ed., Springer, 2006.
- [41] J. Awrejcewicz and M. M. Holicke, *Smooth and Nonsmooth High Dimensional Chaos and the Melnikov-Type Methods*. Singapore: World Scientific Publishing Co. Pte. Ltd, 2007.
- [42] S. Lenci and G. Rega, Heteroclinic Bifurcations and Optimal Control in the Nonlinear Rocking Dynamics of Generic and Slender Rigid Blocks, *International Journal of Bifurcation and Chaos (IJBC)*, Vol. 15, No. 6, 2005, pp. 1901–1918.
- [43] S. Lenci and G. Rega, Higher-Order Melnikov Functions for Single-DOF Mechanical Oscillators: Theoretical Treatment and Applications, *Mathematical Problems in Engineering*, Vol. 2004, No. 2, 2004, pp. 145–168.
- [44] S. Vandepu, B. Verheyden, A. E. Aubert, and S. V. Huffel, Numerical Noise Titration Analysis of Heart Rate Variability in a Healthy Population, in *5th Conference of the European Study Group on Cardiovascular Oscillations*, 2008, pp. 1–4.
- [45] C. Poon, C. Li, and G. Wu, A Unified Theory of Chaos Linking Nonlinear Dynamics and Statistical Physics, *eprint arXiv:1004.1427 [nlin.CD]*, 2010, pp. 1–13.
- [46] J. Gao, J. Hu, X. Mao, and W. Tung, Detecting Low-Dimensional Chaos by the ‘Noise Titration’ Technique: Possible Problems and Remedies, *Chaos, Solitons & Fractals*, Vol. 45, No. 3, 2012, pp. 213–223.
- [47] I. Djurović and V. Rubežić, Chaos Detection in Chaotic Systems with Large Number of Components in Spectral Domain, *Signal Processing*, Vol. 88, No. 9, 2008, pp. 2357–2362.
- [48] A. M. Fraser, Chaos and Detection, *Physical Review E*, Vol. 53, No. 5, 1996, pp. 4514–4523.
- [49] R. Gençay, A Statistical Framework for Testing Chaotic Dynamics via Lyapunov Exponents, *Physica D: Nonlinear Phenomena*, Vol. 89, No. 3–4, 1996, pp. 261–266.
- [50] C. Liu, A Novel Chaotic Attractor, *Chaos, Solitons & Fractals*, Vol. 39, No. 3, 2009, pp. 1037–1045.
- [51] Y. Liu and C. Liqun, *Chaos in Attitude Dynamics of Spacecraft*. Springer, 2013.
- [52] Y. Liu and L. Chen, Chaotic Attitude Motion of a Magnetic Rigid Spacecraft in an Elliptic Orbit and its Control, *Acta Mechanica Sinica (English Series)*, Vol. 19, No. 1, 2003, pp. 71–78.
- [53] L. Cai, J. Zhou, and H. Zhang, Chaos Synchronization of Electro-Mechanical Gyrostat Systems via Time-Delay Feedback Control, in *2011 Fourth International Workshop on Chaos-Fractals Theories and Applications (IWCFTA)*, 2011, pp. 268–272.
- [54] Z.-M. Ge and T.-N. Lin, Chaos, Chaos Control and Synchronization of Electro-Mechanical Gyrostat System, *Journal of Sound and Vibration*, Vol. 259, No. 3, 2003, pp. 585–603.
- [55] O. E. RöSSLer, An Equation for Continuous Chaos, *Physics Letters A*, Vol. 57, No. 5, 1976, pp. 397–398.
- [56] O. E. RöSSLer, An Equation for Hyperchaos, *Physics Letters A*, Vol. 71, No. 2–3, 1979, pp. 155–157.
- [57] P. N. Suganthan, N. Hansen, J. J. Liang, K. Deb, Y.-P. Chen, A. Auger, and S. Tiwari, Problem Definitions and Evaluation Criteria for the CEC 2005 Special Session on Real-Parameter Optimization. Technical Report, 2005.
- [58] E. Kostelich and T. Schreiber, Noise Reduction in Chaotic Time-Series Data: A Survey of Common Methods, *Physical Review. E, Statistical Physics, Plasmas, Fluids, and Related Interdisciplinary Topics*, Vol. 48, No. 3, 1993, pp. 1752–1763.
- [59] S. Jafari, S. M. R. Hashemi Golpayegani, and A. H. Jafari, A Novel Noise Reduction Method Based on Geometrical Properties of Continuous Chaotic Signals, *Scientia Iranica*, Vol. 19, No. 6, 2012, pp. 1837–1842.